Performance Analysis of a Transient-Based Earth Fault Protection System for Unearthed and Compensated Radial Distribution Networks

J. D. Rios Penaloza, A. Borghetti, F. Napolitano, F. Tossani, C. A. Nucci

***Abstract*—This paper deals with the protection against earth faults in distribution networks with unearthed or compensated neutral. A transient-based protection system is proposed and assessed through EMTP simulations. The fault detection algorithm is based on the estimation of the angle between the zero-sequence voltage and current phasors. The estimation is carried out at the dominant transient frequency of the network response within the first milliseconds after the fault. The implementation of an improved filter and a zero-padding process allows for the identification of high resistance faults with a relatively low sampling frequency. An operation zone is proposed and assessed, also for unbalanced or mixed bare and cable line networks. The performances of the protection system are evaluated in a medium voltage distribution network with both unearthed and compensated neutrals through a Monte Carlo method that considers the fault resistance, incidence angle and fault location variations as random variables in the EMTP simulations.**

***Keywords*— Compensated distribution network; Distribution network; Dominant transient frequency; Earth fault protection; Power system faults; Unearthed distribution network.**

I. Introduction

Medium voltage (MV) distribution networks are typically operated in radial configuration due to straightforward control, planning, and design of the protection schemes.

Unearthed and compensated neutral grounding methods are very diffused in MV networks around the world, particularly in Europe. The main advantages are: i) small currents in single phase-to-ground (1PG) faults, ii) the possibility of keeping the faulted system in operation in some cases, and iii) the possibility of fault self-extinction without causing any service interruption. The main disadvantage is due to the overvoltages in the sound phases that may cause the evolution of the fault into a line-to-line one or a cross-country fault. In [1] an average time of 160 ms was estimated before a 1PG-fault evolves to a line-to-line one. A prompt fault clearance would be desired to avoid this phenomenon. Another reason for fast relay operation is the presence of distributed energy resources (DERs), for which connection rules might require DER units to stop feeding the faulty area within a limited time window [2].

In such a context, transient-based protective methods are considered a promising and efficient solution. Different transient-based methods able to detect the faulty section in MV unearthed and compensated neutral networks are documented in the literature. The algorithm presented in [3] evaluates the relationship between the zero-sequence voltage and the zero-sequence charge, estimated as the integral of the zero sequence current. In [4] the protection algorithm computes the zero-sequence power factor estimated from active and reactive powers calculations and in [5] it computes the zero-sequence energy from the integration of the active power. The fault detection techniques presented in [6]–[8] are based on the estimation of the earth-mode impedance that depends on the measure of the early time voltage and current earth modes and on the estimation of the dominant transient frequency. In [9] some of the scenarios in which transient-based protection schemes are prone to fail are reported: i) asymmetrical networks; ii) 0° inception angle, i.e., fault occurrence when the phase voltage is 0; iii) hybrid networks composed of overhead and underground cable lines. These scenarios are analyzed in this paper.

An algorithm based on the detection techniques of [6]–[8] has been presented by the authors in previous papers [10], [11] in which the phase angle between the zero-sequence voltage and current at the dominant transient frequency determines the directionality of the fault. The performances of this algorithm have been assessed for the case of unearthed loop and meshed networks by considering a communication system that interfaces the relays installed at both line-ends. The influence of the communication delays that hinder the protection speed was also analyzed.

This paper focuses on the application in radial networks. The communication between relays is avoided and, with respect to

The authors are with the Department of Electrical, Electronic and Information Engineering, University of Bologna, 40136 Bologna, Italy (e-mail:{juan.riospenaloza3,alberto.borghetti,fabio.napolitano,fabio.tossani,carlo alberto.nucci} @unibo.it)

This work was funded in part by the Italian Ministry for Education, University and Research under the grant PRIN-2017K4JZEE "Planning and flexible operation of micro-grids with generation, storage and demand control as a support to sustainable and efficient electrical power systems: regulatory aspects, modelling and experimental validation".

Paper submitted to the International Conference on Power Systems Transients (IPST2021) in Belo Horizonte, Brazil June 6-10, 2021.

the protection algorithm previously proposed in [10], [11], the analysis of the protection scheme is extended to the case of compensated networks. Moreover, a wider range of fault resistances is considered. The results show the promising detection speed of the protection.

The paper is organized as follows. Section II and Section III describe the studied system, the proposed operation zone, and the protection algorithm. Section IV focuses on the sensitivity analysis. For both types of distribution networks, compensated and unearthed, Section V presents the results of a Monte Carlo analysis in which the fault resistance, location, and inception angle are varied. Section VI concludes the paper.

II. Studied Network

In order to present the characteristics of the developed protection algorithm, we make reference to the network presented in [6] and illustrated in Fig. 1a. It is a typical rural distribution network composed of only overhead lines with the configuration of Fig. 1b. The influence of cable lines is also addressed. The model of the network has been implemented in the Electromagnetic Transient Program EMTP-RV using frequency dependent models for the lines. The network neutral is either unearthed or compensated, depending on the case study.

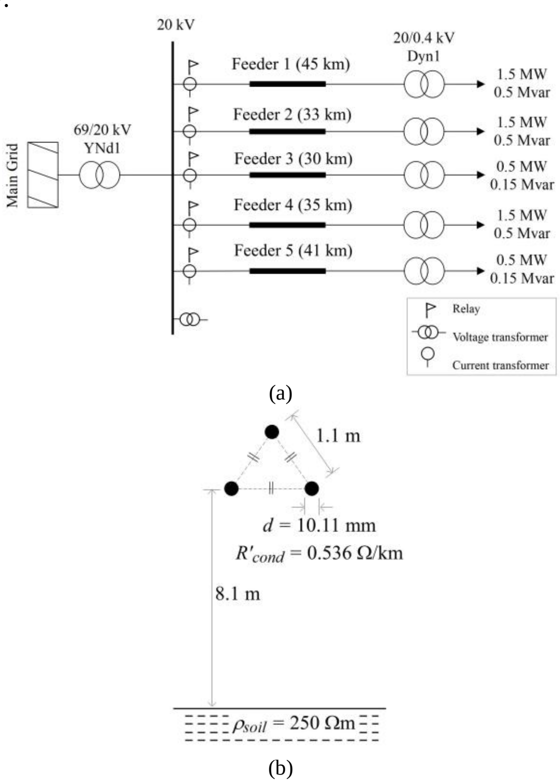

Fig. 1. (a) One line diagram of the considered MV radial distribution network; (b) overhead line geometrical configuration; (c) cable line geometrical configuration. Adapted from [6].

III. The Protection System

When a 1PG fault occurs in an unearthed or compensated network, a transient phenomenon arises, which involves the voltage decrease of the faulty phase and the voltage rise of the sound phases. Following [6]–[8], the charging phenomenon of the sound phases is examined in the proposed fault detection algorithm, corresponding to higher amplitude and lower frequency with respect to the discharging one.

As shown in [7], [11], [12], for the analysis of the zero-sequence current and voltage behavior during the 1PG fault, the network can be reduced to an equivalent circuit including Thevenin's equivalent generators and impedances. Such a circuit can be further reduced to an RLC circuit which inductance and capacitance L_{eq} and C_{eq} affect the dominant transient frequency f_{dom} of the zero-sequence voltage and current:

$$f_{dom} = \frac{1}{2\pi\sqrt{L_{eq}C_{eq}}} \tag{1}$$

As shown in [6], [7], the dominant transient frequencies vary in the range of 100–800 Hz for the network of Fig. 1.

Moreover, (1) shows that: i) for a specific network, long feeders will result in both large equivalent capacitance and inductance, hence in low dominant transient frequencies; ii) due to the large capacitance of underground cables, networks with significant presence of cables also present low dominant transient frequencies [11].

A. *Operation zone*

Assuming a 1PG fault in Feeder 5 with fault resistance R_F, Fig. 2 illustrates the zero-sequence current i_0 path that includes the parasitic capacitances of the healthy phases and, in case of compensated neutral systems, the grounding system of impedance Z_N. Both unearthed and compensated networks are analyzed in the following subsections.

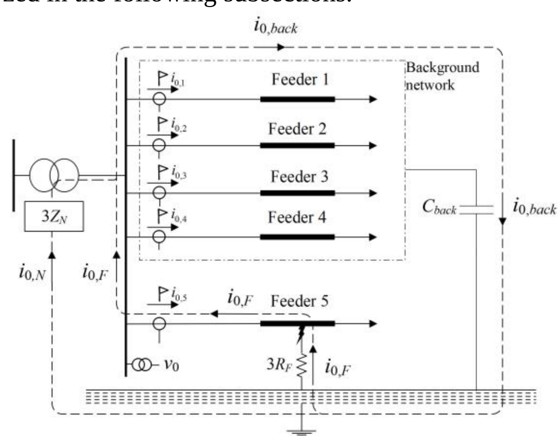

Fig. 2. Circuital representation of the zero-sequence current for a 1PG fault.

a) Unearthed neutral network

When the neutral is unearthed, Z_N is infinite (the capacitive coupling of the transformer to ground is disregarded) and $i_{0,F}$ is equal to the current through the line capacitances, denoted as $i_{0,back}$. If all network resistances and inductances are neglected, the phasor diagram of the zero-sequence quantities is the one of Fig. 3a. If resistances and inductances are considered instead, the phasor diagram becomes the one of Fig. 3b. In any case, there is a significant difference between the angles θ by which the current i_0 lags the voltage v_0 in the faulty feeder and leads it in the healthy ones. Such property is exploited to identify the faulty feeder by defining a proper operation zone delimited by $\theta_{\min}$ and $\theta_{\max}$, as illustrated in Fig. 4.

Fig. 3 shows that two opposite conditions are possible for the faulty feeder: i) entirely capacitive current, for which θ=270°; ii) resistive component is predominant, for which θ=180°. The second condition is considered as a limit case. Based on this analysis and considering a tolerance of 10°, the operation zone proposed for unearthed networks is 170°–280°.

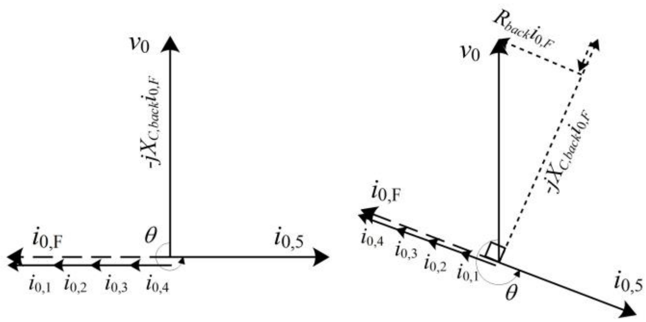

(a) (b)

Fig. 3. Phasor-diagram of the zero-sequence quantities for an unearthed network, (a) neglecting and (b) considering resistances and inductances. R_{back} and $X_{L,back}$ are the equivalent resistance and inductive reactance of the background network. The effect of R_{back} is here exaggerated for illustrative purposes.

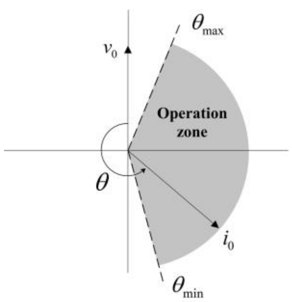

Fig. 4. Operation zone for faulty feeder identification.

b) Compensated neutral network

When a compensated neutral is considered, a variable coil of reactance X_R in parallel to a resistor R_R is connected to the neutral of the network, as illustrated in Fig. 5. If the windings at the secondary side of the substation transformer are wye connected, the star point can be directly grounded through the arc suppression coil; otherwise, if the windings are delta connected, a grounding transformer is used.

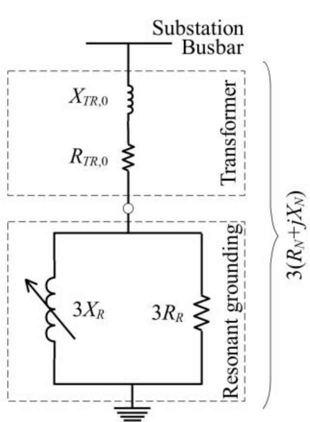

Fig. 5. Zero-sequence circuit of the earthing arrangement in a compensated network. The transformer can be either the main HV/MV substation transformer or the grounding one.

The grade of compensation k is defined as,

$$k = \frac{X_C}{3X_N} \tag{2}$$

where X_C is the capacitive reactance to ground of the entire network ($1/\omega C_0$) and $3X_N$ is the zero-sequence neutral-to-ground reactance at the substation. Neglecting R_R,

$$X_N = X_R + \frac{X_{TR,0}}{3} \tag{3}$$

where $X_{TR,0}$ is the zero-sequence reactance of either the HV/MV transformer or the grounding transformer.

From (2) and (3), the resonant grounding reactance is

$$X_R = \frac{1}{3}\left(\frac{X_C}{k} - X_{TR,0}\right) \tag{4}$$

Since the LV-side of the HV/MV transformer in the studied network is delta-connected, a grounding transformer is considered. The capacitance-to-ground of the overhead line configuration is 4.1 nF/km and, since the network is 184 km long, X_C is equal to 4.21 kΩ. The parameters of the compensated neutral are summarized in Table I, with the typical values adopted from [13]. Three values of compensation degree are considered, namely 0.95, 1 and 1.05, which correspond to the scenarios of under-compensation, perfect compensation, and over-compensation, respectively. The first scenario is the one typically adopted in Italian networks [14], [15].

TABLE I
PARAMETERS OF THE COMPENSATED NEUTRAL ARRANGEMENT

	Parameter values		
$R_{TR,0}$	0.3 Ω		
$X_{TR,0}$	2 Ω		
X_C	4.21 kΩ		
R_R	770 Ω		
	k **= 0.95**	k **= 1.00**	k **= 1.05**
X_R (≈X_N)	1.48 kΩ	1.40 kΩ	1.34 kΩ

The adoption of a transient-based algorithm in compensated networks is facilitated by the high impedance of the coil at high frequencies: during transients the compensated network behaves similarly to the unearthed network [6], [7], [16]. Indeed, from (4), considering a perfectly compensated network, i.e., k = 1, and neglecting $X_{TR,0}$ yields

$$X_R = \frac{X_C}{3} \tag{5}$$

This condition is valid at the utility frequency. Assuming that the transient frequency is m times the utility frequency, i.e., $f_{dom} = m \cdot f$, the inductive reactance increases, and the capacitive reactance decreases of the same factor. Therefore, for the considered range of transient frequencies between 100 and 800 Hz [6], [7], the capacitive current is 4 to 256 times larger than the inductive one when the network is perfectly compensated. The diagrams of Fig. 3 are representative also for compensated networks, even in overcompensation condition. Therefore, an operation zone of 170°–280° is adopted.

B. The protection algorithm

The steps of the proposed protection algorithm are the following: as i_0 could have very low values, particularly for high resistance faults, both i_0 and v_0 are monitored. If one of them exceeds a threshold value, the algorithm starts the process to determine the faulty feeder. The values of i_0 and v_0 are estimated from the measurements of the phase quantities during a time window t_{win}. While in [6] a time window of 2.5 ms is proposed, in this paper a time window of 5 ms is implemented, in order to appraise at least half cycle of the signal corresponding to the minor frequency of the considered range. A Butterworth bandpass digital filter is applied to i_0 and v_0. Consistent to the frequency range, the filter is centered at 450 Hz with a bandwidth of 700 Hz. The Discrete Fourier Transform (DFT) of i_0 is computed to estimate f_{dom}. To obtain the results shown in this paper, the Fast Fourier Transform (FFT) of i_0 is calculated by zero-padding the previous record in order to increase the frequency resolution [17]. This process ensures accurate frequency identification even with relatively low sampling rates, e.g., 8 kHz, achievable by modern digital relays.

The value of f_{dom} corresponds to the peak of the DFT magnitude of i_0. The angles of the relevant phasors to i_0 and v_0 are those at the dominant transient frequency, and angle θ between the phasors is then used to identify the faulty feeder.

IV. Sensitivity analysis

The following analysis illustrates the influence of some parameters of the fault, like the fault resistance, and the protection system, like the filter and the sampling frequency f_s. Moreover, the typical scenarios mentioned in Section I, in which transient-based protection schemes are prone to fail, are assessed. The simulation time step is 10 µs. The protection system parameters are summarized in Table II.

A. Influence of fault resistance and protection characteristics

Two faults are simulated in the middle of phase-*a* of Feeder 5 with a fault resistance of 0 and 10 kΩ respectively, for both networks with unearthed and compensated neutral (k = 0.95). Fig. 6 shows the angles estimated by the protection algorithm. The values agree with the theoretical considerations presented above.

TABLE II
Protection system parameters

Filter center and bandwidth	450 Hz and 700 Hz
t_{win} **(ms)**	5
$v_{0,min}$ **(kV)**	1.0 (5% v_{nom})
$i_{0,min}$ **(A)**	0.5
$\theta_{min} - \theta_{max}$	170° – 280°

Fig. 7 shows the angle estimation as a function of the fault resistance for the unearthed network, for different sampling frequencies. The comparison considers also the fault inception time either as known or unknown in both cases.

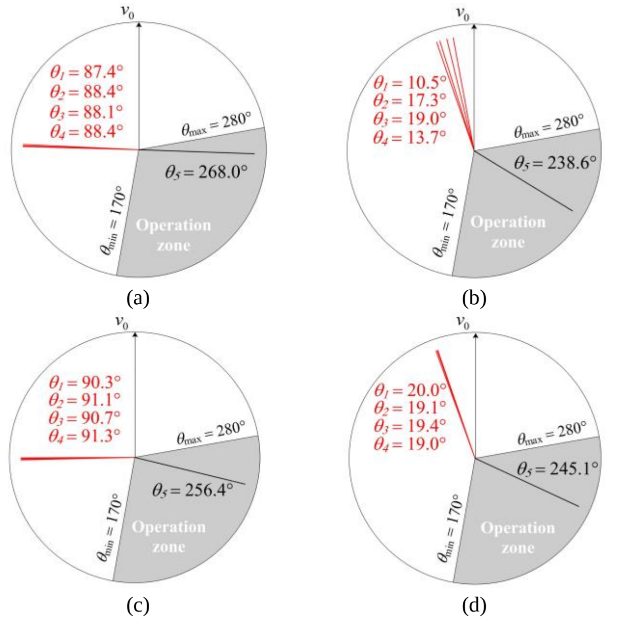

Fig. 6. Angles estimated by the protection algorithm for a fault in the middle of Feeder 5 when the neutral is unearthed (fault resistance equal to (a) 0 and (b) 10 kΩ) and compensated (fault resistance equal to (c) 0 and (d) 10 kΩ).

The comparison shows that the sampling frequency does not considerably affect the estimated angles, due to the zero-padding process. On the other hand, in practical cases the fault time is unknown, and this causes a larger angle variation, particularly at high fault resistances due to different protection triggering mechanism, e.g., for feeder 1 and $R_f \leq 5.75$ kΩ, the current threshold is activated, while for $R_f > 5.75$ kΩ the voltage threshold is activated, leading to a more delayed fault detection. This effect is further illustrated in Fig. 8 which shows the influence of $i_{0,min}$ on the angle estimation. By decreasing $i_{0,min}$, the estimated angle values approach the case in which the fault time is known. Adversely, the relay may pick up in no-fault conditions.

In the following subsections, a 100 kHz sampling rate and known fault time inception are considered to single out and illustrate only the influence of filtering and of critical fault scenarios. In Section V, realistic operating conditions are considered for an overall assessment of the protection performances.

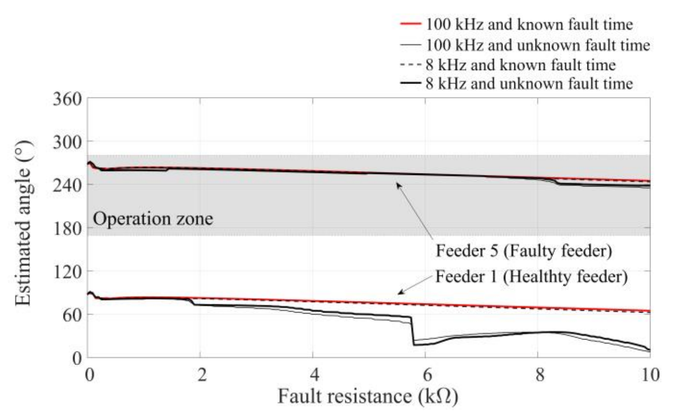

Fig. 7. Influence of fault resistance and other parameters inherent to the protection system on the estimated angles.

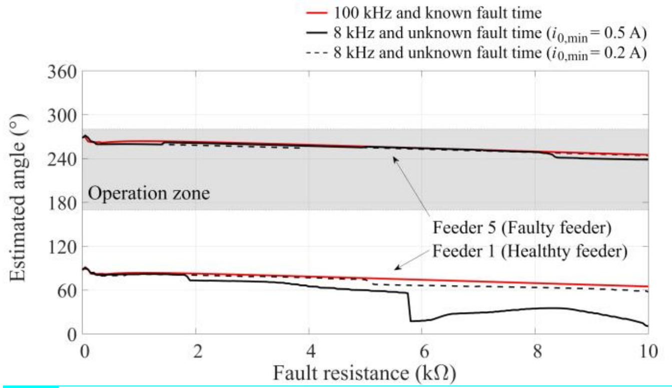

Fig. 8. Influence of $i_{0,min}$ on the estimated angles.

B. *Influence of the filtering process*

One of the main issues with transient-based protection algorithms is that high-resistance faults might damp the transient components of current and voltage, affecting the sensitivity of the relay [18]. Fig. 9 illustrates the DFTs of the raw signals (i.e., without the filtering process) for the same faults analyzed above. For the case with R_F = 0, the dominant transient frequency is clearly identified in the expected range, but for the case with R_F = 10 kΩ it is not. Since the fault resistance value does not significantly affect the transient frequency of the signal but only damps it, a filter can be implemented to the zero-sequence current signal before calculating its DFT. This process improves the f_{dom} identification for high fault resistance values, as illustrated in Fig. 9b.

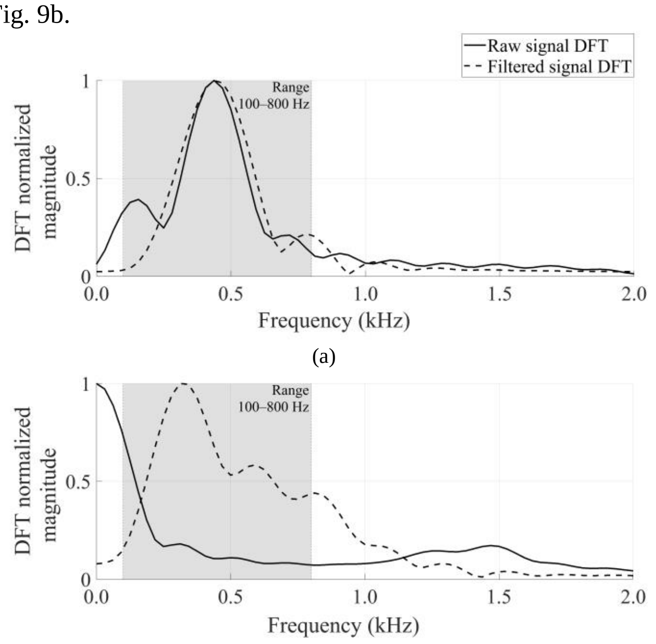

Fig. 9. Filter influence on the identification of f_{dom} for a (a) 0 and (b) 10 kΩ fault resistance.

C. *Critical scenarios*

In the following, the scenarios in which transient-based protection systems might mis-operate are analyzed.

a) *Unbalanced networks*

To increase the difference between the capacitances to earth of the conductors of the network, two capacitances of value $\Delta C/2$ are added at both extremes of phase-*b* in all the feeders of Fig. 1a, such that ΔC is 5% of $3C_0$ of each feeder. Fig. 10 shows the estimated angles when the fault occurs either in phase *a* or *b*. The same filter of Table II is implemented, although the expected frequencies could be lower due to the added capacitances [11]. For this network, the operation zone must be enlarged from 170–280° to 170–315° to obtain a proper behavior. This operation zone is also assessed for the original network. The same calculation is repeated considering a fault angle inception of 0° for both phase *a* and phase *b*. The results are shown in Fig. 10.

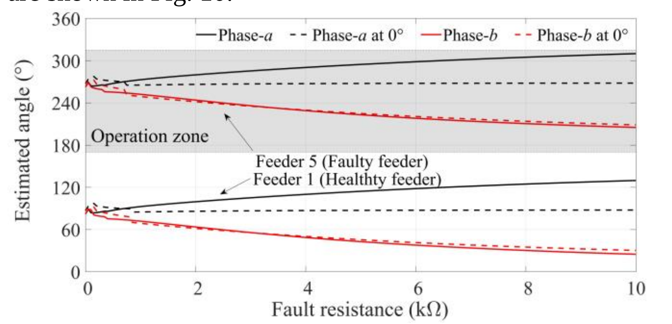

Fig. 10. Estimated angles for faults in the unbalanced network.

b) *Hybrid networks*

For the analysis of a hybrid network, the last 5 km of each feeder are replaced by underground cables with the configuration of Fig. 11a and the cable geometry of Fig. 11c [19]. The estimated angles are shown in Fig. 12 for different fault locations along Feeder 5 and for two values of fault resistance, namely 0 and 10 kΩ. The expected frequencies are lower due to the increased capacitance of cable lines with respect to overhead ones [11].

The same study has been repeated for a trefoil cable line with the configuration of Fig. 11b. The results are shown in Fig. 13. The performance of the protection is not significantly affected by the configuration.

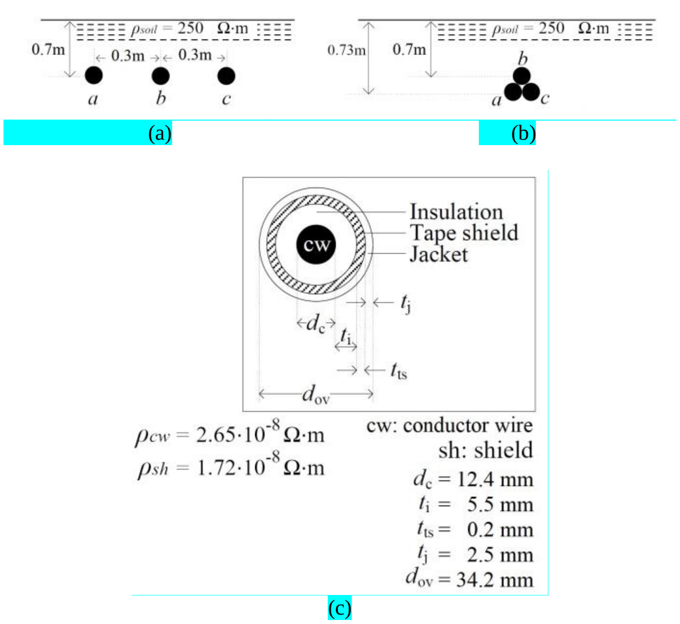

Fig. 11. Cable configuration. (a) Cigré benchmark for European MV distribution networks; (b) trefoil configuration; (c) single cable line geometry for both configurations. Adapted from [19].

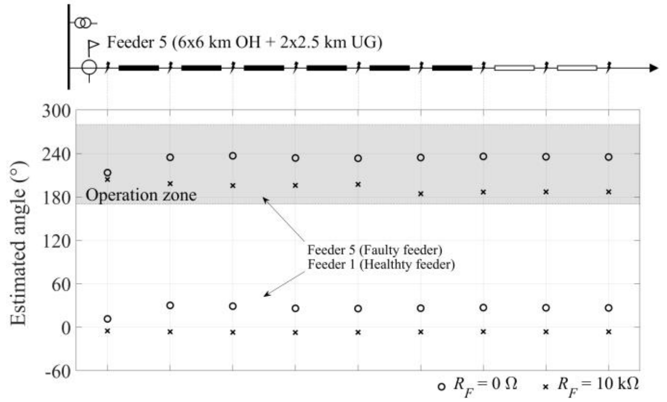

Fig. 12. Estimated angles in a hybrid network with the Cigré benchmark configuration. Feeder 5 is divided in 6 sections of overhead (OH) line each 6 km long, and 2 sections of underground (UG) cable line each 2.5 km long. A fault is simulated at each of these points with 0 and 10 kΩ fault resistance.

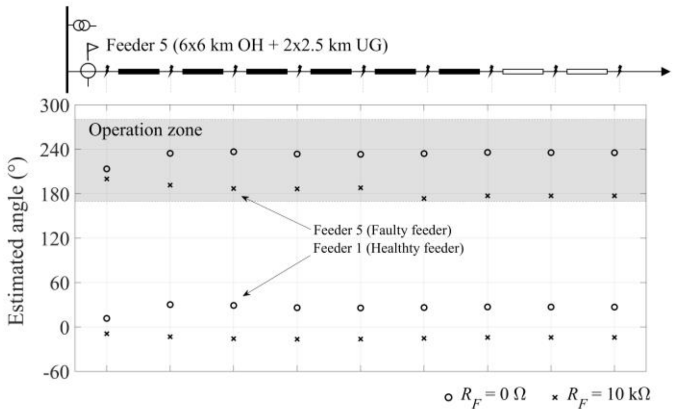

Fig. 13. Estimated angles in a hybrid network with trefoil type cables. Feeder 5 is divided in 6 sections of overhead (OH) line each 6 km long, and 2 sections of underground (UG) cable line each 2.5 km long. A fault is simulated at each of these points with 0 and 10 kΩ fault resistance.

V. Monte Carlo Analysis

To further validate the effectiveness of the protection system and of the proposed operation zone, a Monte Carlo analysis is carried out. A set of 2000 faults randomly distributed within the entire network are simulated, by varying the fault incidence angles over one power frequency period and the fault resistances between 0 and 20 kΩ with the probability distribution reported in [14]. The characteristics of the protection system are the same of Table II and the sampling frequency is 8 kHz. Table III shows the results for the unearthed and compensated network with k = 0.95. The same study was repeated for k = 1 and k = 1.05 and the same results were obtained. All the failure-to-trip cases in the compensated network are related to the threshold value. None is due to an angle misestimation by the algorithm. In these cases, the fault is not detected. If $i_{0,\min}$ is set to 0.25 A, a 0% failure-to-trip and unnecessary trip rates are obtained.

Fig. 14 shows the estimated angles for the healthy and faulty feeders. In 95.8% of cases the angle of the faulty feeder is within the range 250°–280° for the unearthed network and in 96.8% of cases is within 240°–270° for the compensated network. By enlarging the operation zone to 170–315° as required for asymmetrical networks, the same results are obtained.

TABLE III
Monte Carlo Results for Both Unearthed and Compensated Neutral Networks over 2000 Faults

Network	Failure-to-trip rate	Unnecessary trip rate	Mis-operation rate[1]
Unearthed	0.05 %	0.05 %	0.05 %
Compensated	0.65%	0.05%	0.70%

[1]The mis-operation rate is not necessarily the sum of the failure-to-trip and unnecessary trip rates, since sometimes both events occur in a single case.

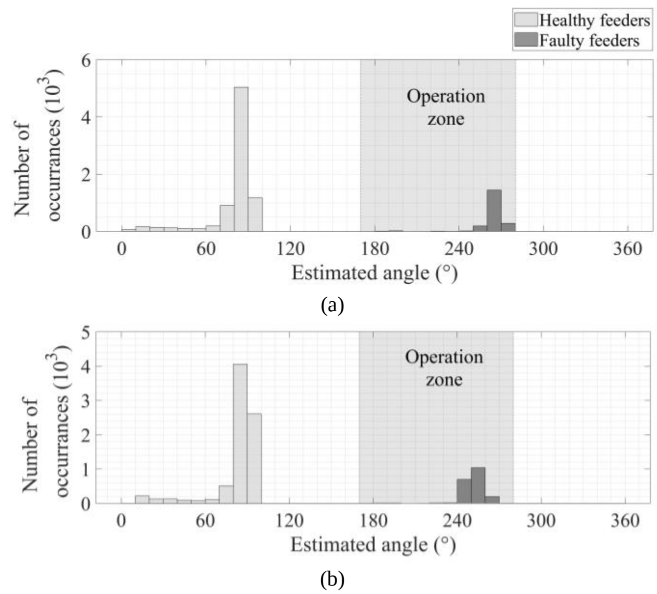

Fig. 14. Estimated angles obtained with the Monte Carlo analysis for both (a) unearthed and (b) compensated networks.

A. Protection speed

The overall protection operating time has the following four components [20].

i) The analog filter delay depends on the filter type and its cutoff frequency, which in turn depends on the sampling frequency. Assuming a second-order filter with cutoff frequency equal to one-third of f_s, such delay can be estimated as $0.75/f_s$ [21].

ii) The sampling latency accounts for the time that the digital filter needs to wait before the first sample is available after the event occurrence and varies between 0 and $1/f_s$.

iii) The digital filter delay is determined by the time window and the input signal magnitude, and its maximum value is equal to the time window.

iv) The protection algorithm processing delay has been estimated from the Monte Carlo analysis and its mean value is 2 ms. It accounts mainly for the DFT computation, including the zero-padding and the angle identification.

Considering the maximum values for the sampling latency and the digital filter delay, the protection operating time is around 7.2 ms from the fault detection instant.

The fault detection time depends mainly on the thresholds and some fault characteristics such as the fault resistance. For the analyzed cases it has a mean value of 0.1 ms with maximum values of 8.1 and 3.6 ms for the unearthed and compensated networks, respectively.

Regarding the compensated network, since its main purpose is to increase the probability of fault self-extinction keeping continuity of service, a prompt operation of the protection would inhibit such advantage. However, the advantage of the proposed protection algorithm lays in the faulty feeder detection during the transient period that might be problematic with steady state signals. Once the faulty feeder has been identified, a time delay can be imposed before sending the trip command to the circuit breaker, depending on the network requirements.

B. Sampling frequency

Since the sampling frequency of some protective devices implemented in distribution systems might be lower than 8 kHz, a further analysis has been carried out to assess the performance of the protection algorithm for lower values of sampling frequency. For such purpose, the Monte Carlo analysis is repeated with 4 and 2 kHz, and the results are reported in Table IV.

The results support the assertion that the influence of the sampling frequency is restrained within some limits.

TABLE IV
MONTE CARLO RESULTS FOR BOTH UNEARTHED AND COMPENSATED NEUTRAL NETWORKS OVER 2000 FAULTS FOR DIFFERENT SAMPLING FREQUENCIES

Network	Sampling frequency	Failure-to-trip rate	Unnecessary trip rate	Mis-operation rate
Unearthed	8 kHz	0.05 %	0.05 %	0.05 %
	4 kHz	0.20 %	0.05 %	0.20 %
	2 kHz	3.45 %	0.45 %	3.85 %
Compensated	8 kHz	0.65 %	0.05 %	0.70 %
	4 kHz	0.65 %	0.00 %	0.65 %
	2 kHz	0.90 %	1.85 %	2.75 %

C. Measurement accuracy

For a preliminary assessment of the influence of the measurement accuracy, a white gaussian noise is added to the zero-sequence voltage and current measured signals. The obtained results are shown in Table V, in which the noise is represented in terms of ratio of the amplitude values of noise with respect to the signal. The results without noise are also shown.

TABLE V
MONTE CARLO RESULTS FOR BOTH UNEARTHED AND COMPENSATED NEUTRAL NETWORKS OVER 2000 FAULTS FOR DIFFERENT RATIOS OF NOISE

Network	Ratio of noise	Failure-to-trip rate	Unnecessary trip rate	Mis-operation rate
Unearthed	0 %	0.05 %	0.05 %	0.05 %
	1 %	0.05 %	0.05 %	0.05 %
	3 %	0.60 %	0.40 %	0.95 %
Compensated	0 %	0.65 %	0.05 %	0.70 %
	1 %	0.65 %	0.05 %	0.70 %
	3 %	0.75 %	0.05 %	0.80 %

According to these results, the noise has a limited impact on the protection performance. However, other causes of measurement inaccuracies could be examined.

D. Prevalence of cable lines

In this case study, feeders 1 to 4 of the network of Fig. 1a of the manuscript are underground cables and feeder 5 is an overhead line (i.e., 77.7% of the network is constituted by cable lines and 22.3% is constituted by overhead lines). The analysis is carried out only for the sake of the protection performance assessment, disregarding other issues, such as voltage constraint violations, due to the presence of long cable lines. The Monte Carlo analysis has been carried out with the same characteristics as before, i.e., faults are randomly distributed within the entire network varying the fault incidence angles over one power frequency period and the fault resistances between 0 and 20 kΩ with the probability distribution reported in [14]. The characteristics of the protection system are the same of Table II and the sampling frequency is 8 kHz. The results are summarized in Table VI and the distribution of the estimated angles for this network is reported in Fig. 15. The results present a satisfactory protection performance.

TABLE VI
MONTE CARLO RESULTS FOR THE UNEARTHED NEUTRAL NETWORK PREVALENTLY COMPOSED BY UNDERGROUND CABLES

Network	Failure-to-trip rate	Unnecessary trip rate	Mis-operation rate
Unearthed	1.30 %	0.25 %	1.40 %

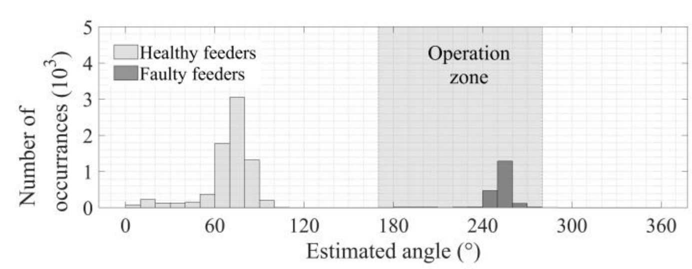

Fig. 15. Estimated angles obtained with the Monte Carlo analysis for a network prevalently composed by underground cables

CONCLUSIONS

The protection system dealt with in this paper is based on directional relays which implement a transient fault detection algorithm. The algorithm identifies the faulty feeder by estimating the angle between the zero-sequence voltage and current phasors at the dominant transient frequency. The performances of the protection system are analyzed for the earth fault protection of both unearthed and compensated distribution networks, both having radial configuration.

The carried-out sensitivity analysis shows that a fast fault detection is important to contain the deviation of the estimated angles with respect to the expected values, particularly for high resistance faults. Due to a zero-padding process during the DFT computation of the zero-sequence current, the sampling frequency does not produce a significant impact on the protection performance, hence a sampling frequency of 8 kHz, attainable by modern relays, has been implemented. The performance has been assessed for lower sampling frequencies too, namely 4 and 2 kHz, with satisfactory results.

The protection system has been assessed for scenarios in which transient-based protection systems are prone to mis-operate. In systems with high degree of asymmetry, the operation zone might need to be enlarged. While an operation zone within 170–280° is adequate for the original system, an operation zone within 170–315° is required for the asymmetrical one. However, the latter operation zone is adequate also for the original system. Additionally, the presence of underground cable lines does not particularly affect the performances of the protection system.

The assessment of the performances of the protection system in several different cases has been carried out by Monte Carlo simulations, varying the fault resistance, the fault incidence angle, and the fault location within the network. The results satisfy the requirements with a negligible mis-operation rate, which is lower than 0.05% in unearthed networks and about 0.65% in compensated networks. The mis-operation rate in compensated networks further decreases by reducing the zero-sequence current threshold.

The expected protection speed is particularly satisfactory. The fault detection time has a mean value of 0.1 ms, while the protection operating time is around 7.2 ms.

According to a preliminary analysis, the noise added to the measurements has a limited impact on the protection performance.

References

[1] S. Hänninen and M. Lehtonen, "Characteristics of earth faults in electrical distribution networks with high impedance earthing," *Electr. Power Syst. Res.*, vol. 44, no. 3, pp. 155–161, 1998.

[2] Institute of Electrical and Electronics Engineers, "IEEE Std. 1547-2018. Standard for Interconnection and Interoperability of Distributed Energy Resources with Associated Electric Power Systems Interfaces," *IEEE Std 1547-2018 (Revision of IEEE Std 1547-2003)*. 2018.

[3] T. Henriksen, "Faulty feeder identification in high impedance grounded network using charge-voltage relationship," *Electr. Power Syst. Res.*, vol. 81, no. 9, pp. 1832–1839, 2011.

[4] P. Balcerek, M. Fulczyk, J. Izykowski, E. Rosolowski, and P. Pierz, "Centralized substation level protection for determination of faulty feeder in distribution network," in *IEEE Power and Energy Society General Meeting*, San Diego, CA, USA, 2012.

[5] M. Loos, S. Werben, M. Kereit, and J. C. Maun, "Fault direction method in compensated network using the zero sequence active energy signal," in *IEEE EuroCon 2013*, 2013.

[6] M. F. Abdel-Fattah and M. Lehtonen, "A New Transient Impedance-Based Algorithm for Earth Fault Detection in Medium Voltage Networks," in *International Conference on Power Systems Transients*, 2009.

[7] M. F. Abdel-Fattah and M. Lehtonen, "Transient algorithm based on earth capacitance estimation for earth-fault detection in medium-voltage networks," *IET Gener. Transm. Distrib.*, vol. 6, no. 2, pp. 161–166, 2012.

[8] M. F. Abdel-Fattah and M. Lehtonen, "A transient fault detection technique with varying fault detection window of earth modes in unearthed MV systems," in *6th International Conference - Power Quality and Supply Reliability*, 2008.

[9] K. Pandakov, H. K. Høidalen, and J. I. Marvik, "Misoperation analysis of steady-state and transient methods on earth fault locating in compensated distribution networks," *Sustain. Energy, Grids Networks*, vol. 15, pp. 34–42, 2018.

[10] J. D. Rios Penaloza, A. Borghetti, F. Napolitano, F. Tossani, and C. A. Nucci, "Performance Analysis of a Communication-Supported Earth Fault Protection System of Medium Voltage Loop and Meshed Networks," in *18th EEEIC Environment and Electrical Engineering International Conference*, Palermo, Italy, Italy, 2018, pp. 1314–1319.

[11] J. D. Rios Penaloza, A. Borghetti, F. Napolitano, F. Tossani, and C. A. Nucci, "A New Transient-Based Earth Fault Protection System for Unearthed Meshed Distribution Networks," *IEEE Trans. Power Deliv. (Early Access)*, 2020.

[12] S. Hänninen, "Single phase earth faults in high impedance grounded networks: Characteristics, indication and location," *VTT Publ.*, 2001.

[13] ENEL Distribuzione S.p.A., "Criteri di protezione della rete MT di distribuzione - DK 4451 Ed. 2.1," 2005.

[14] A. Cerretti, F. M. Gatta, A. Geri, S. Lauria, M. MacCioni, and G. Valtorta, "Ground fault temporary overvoltages in MV networks: Evaluation and experimental tests," *IEEE Trans. Power Deliv.*, 2012.

[15] M. Brenna, E. De Berardinis, L. Delli Carpini, P. Paulon, P. Petroni, G. Sapienza, G. Scrosati, and D. Zaninelli, "Petersen coil regulators analysis using a real-time digital simulator," *IEEE Trans. Power Deliv.*, 2011.

[16] M. Lehtonen, R. J. Millar, and C. J. Kim, "The Impact of the Distribution Network Type and Configuration on the Transient Behavior of the Fault and Neutral Points during Earth Faults," in *International Conference on Power Systems Transients*, Delft, Netherlands, 2011.

[17] J. Arrillaga and N. R. Watson, *Power system harmonics*. John Wiley & Sons Ltd., 2003.

[18] J. Roberts, H. J. Altuve, and D. Hou, "Review of ground fault protection methods for grounded, ungrounded, and compensated distribution systems," *27th Annu. West. Prot. Relay Conf.*, 2001.

[19] CIGRE Working Group C4.605, "Benchmark Systems for Network Integration of Renewable and Distributed Energy Resources," CIGRE, Paris, France, Tech. Rep. C6.04.02, 2014.

[20] H. J. Altuve, K. Zimmerman, and D. Tziouvaras, "Maximizing line protection reliability, speed, and sensitivity," in *69th Annual Conference for Protective Relay Engineers*, College Station, TX, USA, 2016, pp. 1–28.

[21] S. J. Elliott, *Signal Processing for Active Control*, 1st ed. Academic Press, 2001.